J. Braz. Chem. Soc., Vol. 19, No. 1, 157-161, 2008.
Printed in Brazil - ©2008 Sociedade Brasileira de Química
0103 - 5053 $6.00+0.00

Article

Computer-based Simulation of High-Temperature Corrosion Phenomena

Vicente Braz Trindade,[a] Ulrich Krupp[b] and Hans-Jürgen Christ[a]*

[a]*Institute for Materials Science, Universität Siegen, Paul-Bonatz Str. 9-11, 57076 Siegen, Germany*
[b]*FH Osnabrück, University of Applied Sciences, Germany*

O objetivo deste artigo é introduzir uma ferramenta para simulação computacional, capaz de prever a vida útil de componentes que operam em condições corrosivas tais como oxidação, nitretação e carbonetação em temperaturas elevadas. Diferentes classes de materiais (aços ferríticos, aços austeníticos e ligas de níquel) foram expostas a diferentes atmosferas e temperaturas. O software desenvolvido para simulação de corrosão interna em temperaturas elevadas utiliza a técnica numérica de diferenças finitas para descrever a cinética de corrosão e o conceito de equilíbrio termodinâmico local para tratar a estabilidade das fases. Para isto, um link entre o ambiente MATLAB e a sub-rotina termoquímica ChemApp foi criado. Usando esta ferramenta, cinéticas de oxidação, nitretação e carbonetação foram calculadas levando em consideração a microestrutura das ligas, distinguindo precipitação no interior do grão e no contorno do grão. Foi observada uma excelente correlação entre os resultados experimentais e aqueles obtidos através de simulação computacional.

The aim of this paper is to introduce a computer simulation tool, which is designed for prediction of service-life of components operating under corrosive conditions such as carburization, oxidation and nitridation at high-temperature. Different classes of materials (low-Cr ferritic steels, austenitic steels and Ni-base superalloys) were exposed at temperatures between 550 °C and 1000 °C to different corrosive atmospheres (carburizing, oxidizing and nitriding). The tool for the prediction of internal/inwards corrosion processes at high-temperatures makes use of the numerical finite-difference technique to treat diffusional kinetics on the one hand and the concept of local equilibrium thermodynamics on the other hand. For this purpose, a link has been established between the numerical environment of MATLAB and the thermodynamic library ChemApp. Using this new tool, the kinetics of nitridation, oxidation and carburization processes were predicted numerically taking the material's microstructure into consideration by distinguishing between precipitation along the grain boundaries and within the grain interior. Excellent agreement between experimental observations and simulation results revealed the high potential of the computer modeling for application to complex corrosion processes.

Keywords: thermodynamics and diffusion simulation, oxidation, nitridation, carburization, finite-difference method

Introduction

Many industrial processes involve chemical reactions that are thermally activated, consequently, operated at high-temperature conditions. In the petrochemical industry, for instance, large hydrocarbon molecules have to be cracked into small molecules, e.g., methane, ethylene, etc. These reactions take place in steel tubes located in a gas-fired furnace at temperatures up to 900 °C. The surfaces of the tubes (reaction chambers) are exposed to high carbon activities. The soluble carbon can diffuse into the steel forming internal carbides.[1] Due to the higher carbon diffusion along grain boundaries, precipitation occurs preferentially intercrystalline. This phenomenon called carburization shortens the service-life of the tubes by degradation of its mechanical properties.

In the power generation industry, steels are also used as boiler materials. The operation temperature in the different

*e-mail: vicentebraz@yahoo.com.br

components of a boiler system varies from 400 to 650 °C. The tubes are exposed to a outer oxidizing atmosphere and internally to very high pressures (up to 300 bar). Therefore, the performance of the boiler components is strongly dependent on their resistance to oxidation, since the formation of oxide scales causes a reduction of the thickness of the tube walls. Usually, the oxidation rate of steels is strongly dependent on their chromium content, because chromium has a very high affinity to oxygen, *i.e.*, chromium oxide (Cr_2O_3) has a high thermodynamic stability. Its very low defect density results in an adherent, slow-growing, and protective scale.[2]

In the aeronautic industry, critical components subject to failure caused by high temperature corrosion are the turbine blades, which are made of Ni-base superalloys. The very high temperatures (up to 1100 °C) at which the turbine blades are used represent very aggressive conditions, even when a chromia scale is formed on the surface. Under these conditions, elements such as oxygen and/or nitrogen can penetrate within the oxide scale and dissolve in the alloys causing internal precipitation of oxides and/or nitrides reducing the service-life of the blades.[3]

The stability of the different phases such as carbides, oxides and nitrides can be evaluated by their thermodynamic properties. However, the existence of complex solid solution such as some carbides and oxides containing different metallic elements in its sublattices, a properly prediction of phase equilibrium becomes reasonable when using computational thermochemistry. Besides thermodynamics, the kinetics of the corrosion process has to be evaluated by considering that the most of the corrosion phenomena are controlled by solid state diffusion. Therefore, the diffusion of the different species participating in the corrosion phenomena must be taken into account and considering the high diffusivity along grain boundaries.

In this paper both thermodynamics and diffusion characteristics of the different corrosion degradation phenomena are considered. Computational thermodynamics is done by means of the powerful programmable thermochemical subroutine ChemApp by GTT Technologies using tailored thermodynamic data bank for steels and Ni-base superalloys. The kinetic calculations are performed by solving the diffusion differential equation in one- and two-dimentional cases with help of the finite-difference method. A computer tool for description of high-temperature corrosion phenomena is presented and the simulation results are compared with that experimentally observed.

Experimental

In this paper three classes of materials are considered: (*i*) low-Cr ferritic steels used in power plant, (*ii*) austenitic steels used in petrochemical industry and (*iii*) Ni-base superalloys used in the aeronautic industry. The low-alloy steels have chromium content from 0.5 wt.% to 2.25 wt.% and they were oxidized in laboratory air at 550 °C. The austenitic steel containing 16.8 wt.% of Cr and 7.41 wt.% of Ni was exposed to an oxygen-free He atmosphere containing 1 vol % of methane at 850 °C. One of the Ni-base superalloys (IN625) was exposed to laboratory air at a temperature range between 850 °C and 1000 °C. The Ni-base superalloy Nicrofer7520Ti was exposed to nitriding/oxidizing atmospheres at 1000 °C. The chemical compositions of the materials used are given in Table 1.

The materials were isothermally exposed to high temperatures and the mass change during the different corrosion processes was recorded using a microbalance with a resolution of 10^{-5} g connected to a computer. The oxide, nitride and carbide phases were analyzed using scanning electron microscopy (SEM) in combination with energy-dispersive X-ray spectroscopy (EDX).

Results and Discussion

Generally, the driving force of high-temperature corrosion processes can be separated into (*i*) transport mechanisms, *i.e.*, solid-state diffusion, and (*ii*) thermodynamics of chemical reactions. The commonly used, phenomenological way to treat diffusion processes is the application of a second-order partial differential

Table 1. Chemical compositions (in wt.%) of the materials used

Alloy	C	Cr	Mo	Ti	Al	Si	Ni	Fe
71518	0.07	0.55	---	---	---	---	---	bal.
NrX60	0.06	1.44	---	---	---	---	---	bal.
2.25Cr1Mo	0.09	2.25	1	---	---	---	---	bal.
AISI 301	0.108	16.8	0.32	---	0.033	0.98	7.41	bal.
IN625	0.01	19.0	8.9	0.28	0.24	1.20	bal.	2.80
Nicrofer7520	0.02	20.2	---	2.7	1.6	---	bal.	0.2

equation (Fick's 2nd law) formulating a relationship between the derivative of the concentration of a species c after the time t and its gradient by means of the location- and temperature-dependent diffusion coefficient D.

$$\frac{\partial c}{\partial t} = D\frac{\partial^2 c}{\partial x^2} \quad (1)$$

The use of analytical solutions for equation 1 to describe the corrosion phenomena in complex situations is widely limited. Therefore, numerical methods, e.g. the finite-difference technique, have the advantage that the concentrations of the species can be calculated in discrete steps of time and location. Such approaches the incorporation of computational thermodynamics in each of the discrete steps.

The basic idea of the finite-difference method to solve partial differential equations is to replace spatial and time derivatives by suitable approximations and then to numerically solve the resulting difference equations. In other words, instead of solving for $c(x,t)$ with x and t continuous, it is solved for $c_{i,j} = (x_i, t_j)$, where $x_i = i\Delta x$ and $t_j = j\Delta t$. Thus, if all the concentrations are known at time t_j, then one step of the process is to determine them at time $t_{j+1} = t_j + \Delta t$. If this can be done, then, given the initial state, the concentration profiles can be determined for all following time steps. Using the Crank-Nicolson technique,[4] equation 1 can be approximated as follows:

$$\frac{\partial c}{\partial t} \cong \frac{c_i^{j+1} - c_i^j}{\Delta t} \quad (2)$$

$$\frac{\partial^2 c}{\partial x^2} \cong \frac{1}{2}\left(\frac{c_{i+1}^{j+1} - 2c_i^{j+1} + c_{i-1}^{j+1}}{(\Delta x)^2} + \frac{c_{i+1}^{j} - 2c_i^{j} + c_{i-1}^{j}}{(\Delta x)^2}\right) \quad (3)$$

By combining equation 2 and equation 3 the concentrations c_i^{j+1} of the diffusing species for the location step i and the time step $j+1$ are calculated from the neighbouring concentrations according to the equation 4 and schematically represented in Figure 1.

$$c_i^{j+1} = c_i^j + \frac{D\Delta t}{2(\Delta x)^2}\left[\left(c_{i+1}^{j+1} + c_{i+1}^{j}\right) - 2\left(c_i^{j+1} + C_i^{j}\right) + \left(c_{i-1}^{j+1} + c_{i-1}^{j}\right)\right] \quad (4)$$

For separation of diffusion along grain boundaries from that in the bulk, a two-dimensional calculation is required. In this case, the diffusion coefficient D is treated as a matrix containing the diffusion coefficients of the diffusing species as a function of the position x and y. This allows changing the diffusion coefficient locally, e.g., along grain boundaries.

Equation 1 is solved for all species participating in the corrosion process and stepwise for the complete reaction time $p\ \Delta t$ using the commercial simulation environment MATLAB according to the schematic representation in Figure 1 (simplified for one-dimensional diffusion). To account for possible chemical reactions of the ongoing corrosion process, the calculated concentrations at c_i^{j+1} must be corrected according to the local thermodynamic equilibrium. This becomes possible by transferring the concentration c_i^{j+1} into the thermodynamic subroutine ChemApp. ChemApp is based on a numerical Gibbs' energy minimization routine in combination with tailor-made databases. The excessive computation time was drastically reduced by using the parallel computing system PVM (parallel virtual machine).[5-7] Using this computation methodology the thermodynamic equilibrium calculations are distributed to individual thermodynamic workers according to the schematic representation in Figure 1.

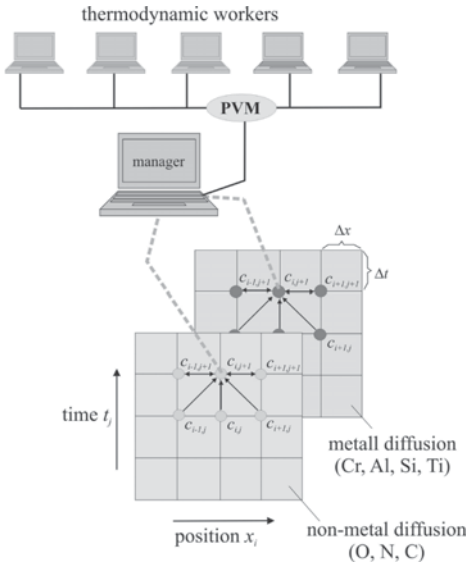

Figure 1. Schematic representation of the finite-difference technique (implicit Crank-Nicolson approach) in combination with the thermodynamic subroutine ChemApp.

On the surface of the low-Cr ferritic steels a thick oxide scale was formed following parabolic rate law kinetics, strongly dependent on the microstructure (grain size) of the alloy. It has been shown by Trindade *et al.*[6] that this oxide scale was composed of two layers: (*i*) an outer layer of magnetite (Fe_3O_4) and hematite (Fe_2O_3), which grows by outwards diffusion of iron and (*ii*) an inner layer of spinel ($FeFe_{2-x}Cr_xO_4$) with stoichiometry varying from x=0 (pure magnetite-Fe_3O_4) up to x=2 (normal spinel-$FeCr_2O_4$). The growth of the inner layer is determined by fast diffusion of oxygen along alloy grain boundaries resulting in an intergranular oxidation mechanism (see Figure 2a).

The application of the developed simulation tool to the oxidation of low-Cr steels is demonstrated by calculations of

the inner oxide scale growth. To account for the intercrystalline oxidation mechanism, the diffusion of oxygen and chromium along alloy grain boundaries was separated from that in the bulk. Figure 2b shows the simulated concentration profiles of Fe_3O_4 and the complete spinel $FeCr_2O_4$. The high oxygen grain boundary diffusivity cause the primary formation of oxides along grain boundaries and the lateral diffusion from the grain boundary in the interior of the grain determines the kinetics of the inward oxidation of this steel grade.

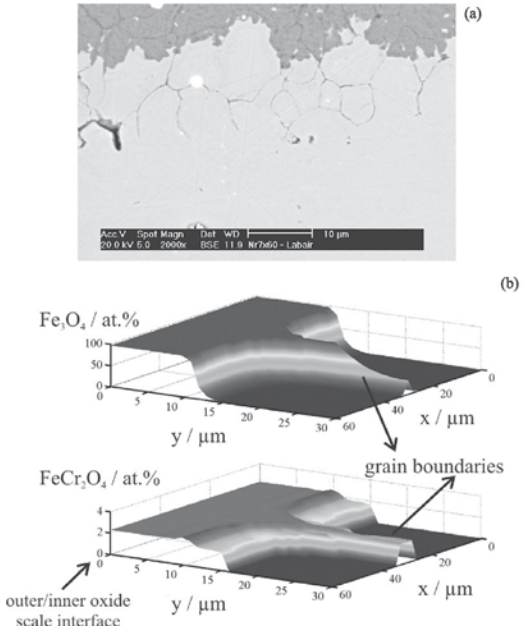

Figure 2. Oxide scale formed on low-Cr steel with a grain size of 30 µm at 550 °C exposed to laboratory air: (a) detail of the formation of inner oxide scale and (b) simulation of the intergranular growth of the inner scale.

The exposure of the austenitic steel to a carburizing atmosphere causes the dissolution of carbon in the alloy and its diffusion into the alloy leads to formation of carbides. The high affinity of chromium and iron to carbon causes the formation of carbides such as Me_7C_3 and $Me_{23}C_6$, where Me denotes the metallic component (Fe and Cr). The high diffusivity of carbon along alloy grain boundaries causes the formation of the most stable $Me_{23}C_6$ carbide along grain boundaries, which transforms to Me_7C_3 as the carbon activity increases. Figure 3a shows the formation of $Me_{23}C_6$ formed during the first stage of exposure. An external oxide scale was not formed due to the very low oxygen partial pressure in the atmosphere.

Figure 3b shows the concentration profiles of the main species involved in the carburization process. The formation of $Me_{23}C_6$ along grain boundaries and in the grain interior as well as the depletion of iron and chromium in the matrix and along alloy grain boundaries are in good agreement with experimental results.

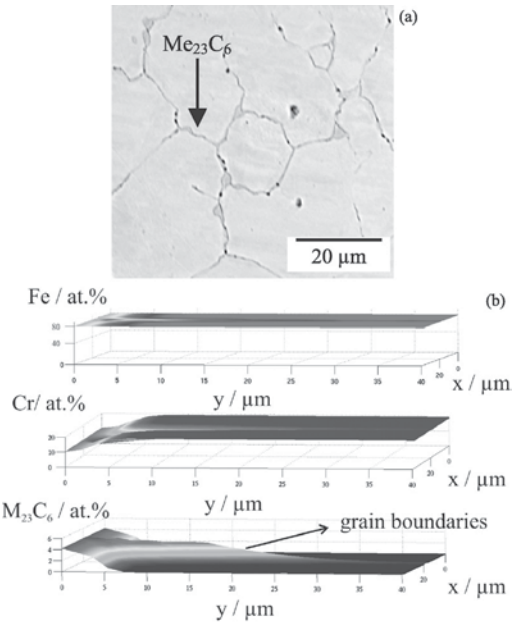

Figure 3. Initial stage of carbide formation in austenitic steel at 850 °C during exposure to an He atmosphere containing 1 vol.% of methane for 10h: (a) cross section and (b) simulated concentration profiles.

The high Cr concentration in the alloy IN625 causes the formation of an external chromium oxide scale (Cr_2O_3) during exposure to an oxidizing atmosphere at temperature range between 850 °C and 1000 °C.[8] Beside the superficial Cr_2O_3 scale, internal oxides can be observed (see Figure 4a). The internal oxidation zone is composed of intergranular aluminum oxide (Al_2O_3). Simulation of this internal oxidation process is shown in Figure 4b. Aluminum depletion along grain boundaries as a consequence of aluminum oxide formation is clearly demonstrated by faster diffusion of oxygen along alloy grain boundaries.

During exposure of the Ni-base alloys Nicrofer7520Ti to an atmosphere containing nitrogen can cause diffusion of dissolved nitrogen into the alloy leading to the formation of nitrides, e.g., TiN, AlN, CrN and Cr_2N. However, the formation of chromium nitrides occurs only for high nitrogen partial pressures and Cr concentrations. Figure 5a shows the formation of an internal corrosion zone (oxidation + nitridation) formed in Nicrofer7520Ti exposed to laboratory air at 1000 °C. The thermodynamically most stable nitride (TiN) was formed on the reaction front while the the less stable nitride (AlN) was formed near to the sample surface as observed by Krupp and Christ[3] Due to the presence of oxygen in the atmosphere, both nitrides and oxides are formed, according to their thermodynamic stabilities. By computer simulation the simultaneous formation of oxides and nitrides and their respective sequence of formation could be shown in Figure 5b.

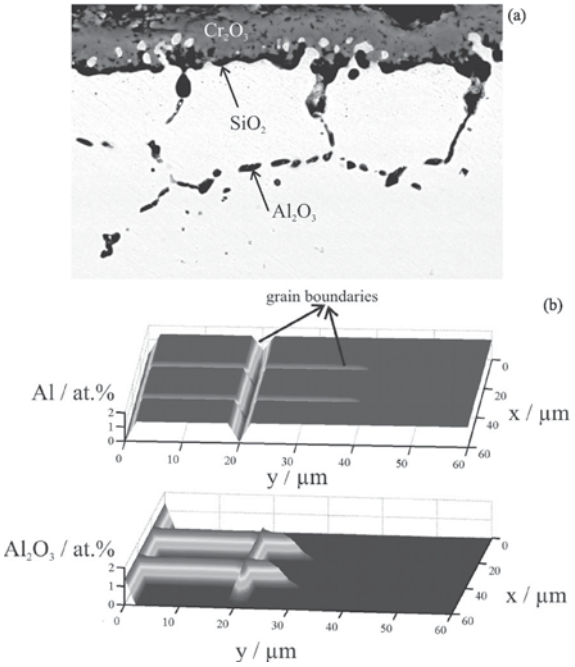

Figure 4. Cr_2O_3 scale and internal oxidation zone (Al_2O_3) formed during exposure of the alloy IN625 to laboratory air at 1000 °C: (a) cross section observation[8] and (b) simulated concentration profile of intergranular Al_2O_3 formation.

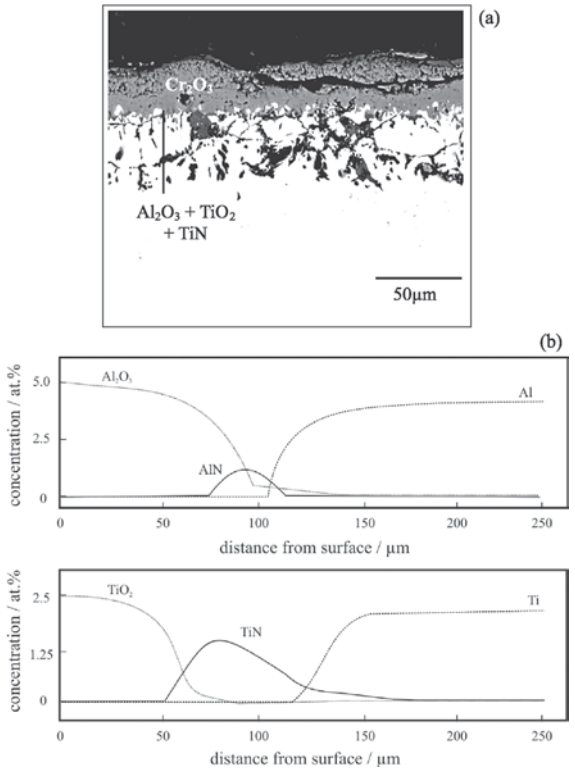

Figure 5. Corrosion of the Ni-base alloy Nicrofer7520Ti at 1000 °C after 100 h of exposure to laboratory air: (a) simultaneous formation of oxides and nitrides and (b) one-dimensional simulated concentration profiles of the species involved in the corrosion process.

Conclusions

In this paper, a computer-based simulation was introduced and applied for three industrial relevant systems, namely, (*i*) oxidation of low-chromium ferritic steels, (*ii*) carburization of austenitic steels, and (*iii*) simultaneous internal nitridation and oxidation of Ni-base superalloys. The versatility of the developed simulation tool allows to perform complex thermodynamic equilibrium calculations by means of the thermodynamic subroutine ChemApp, which is coupled with diffusion calculations. The diffusion differential equation was solved for one- and two-dimensional cases using the MATLAB environment. Diffusion along grain boundaries was separated from that in the bulk of the alloy. A very good agreement between experimental observations and simulation results has proven the high performance of the computer modeling. Therefore, it can be applied for prediction of service life of metallic components used in different atmospheres at high-temperatures as well as for materials selection.

Acknowledgments

This research has been supported by the EU project OPTICORR and by the Brazilian Federal Agency for Support and Evaluation of Graduate Education (CAPES) through a fellowship to one of the authors (V. B. Trindade).

References

1. Grabke, H. J.; *Mater. Corros.* **1998**, *49*, 303.
2. Kofstad, P.; *High Temperature Oxidation of Metals*, Electrochemical Society: London, 1966.
3. Krupp, U.; Christ, H. -J.; *Metall. Mater. Trans. A* **2000**, *31*, 47.
4. Crank, J.; *The Mathematics of Diffusion*, Clarendon Press: Oxford, 1986.
5. Krupp, U.; Trindade, V. B.; Schmidt, P.; Christ, H. J.; Buschmann, U.; Wiechert, W.; *Mater. Corros.* **2006**, *57*, 263.
6. Trindade, V. B.; Krupp, U.; Christ, H.-J.; *Opticorr Guide Book*, VTT Research Center: Finland, 2005.
7. Trindade, V. B.; *Ph.D. Thesis*, Universität Siegen, 2006.
8. Trindade, V. B.; Krupp, U.; Wagenhuber, Ph. E. G.; Christ, H. J.; *Mater. Corros.* **2005**, *56*, 785.

Received: April 26, 2007
Published on the web: January 30, 2008